Electron Paramagnetic Resonance Evidence for Electrochemical Formation of $Mo^{V}O_2$, *cis*-$Mo^{V}O$(OH), $Mo^{V}O$(S) and *cis*-$Mo^{V}O$(SH) Centers

CAROL J. HINSHAW and JACK T. SPENCE

Department of Chemistry and Biochemistry, Utah State University, Logan, Utah 84322-0300, U.S.A.

(Received February 22, 1986)

Recent EPR and EXAFS studies indicate the presence of an OH ligand at the Mo center in the reduced states of sulfite oxidase (SO) and nitrate reductase (NR), and an SH ligand in the reduced states of xanthine oxidase (XO) and xanthine dehydrogenase (XDH) [1–3]. The observed superhyperfine coupling of a ^1H in the Mo(V) EPR signal of these enzymes is believed to arise from the OH or SH proton* [1, 3].

The only nonenzymatic ^1H EPR coupling of an OH proton to Mo(V) is that observed upon photolysis of single crystals of $[RNH_3]_6[Mo_7O_{24}]\cdot 3H_2O$ [4], while no nonenzymatic Mo(V) SH proton couplings have been reported.

We have synthesized new *cis*-dioxo-Mo(VI) complexes (**I–III**) with sterically bulky ligands which undergo one electron reversible electrochemical reduction on both the cyclic voltammogramic and coulometric time scales to give Mo(V) monomers [5]. We report here EPR evidence for the formation of $[MoO_2L]^-$, *cis*-MoO(OH)L, $[MoO(S)L]^-$ and *cis*-MoO(SH)L species obtained in solution by electrochemical reduction of these MoO_2L complexes under appropriate conditions. The X-ray structure of **I** indicates a *cis*-dioxo structure with approximate C_2 symmetry [6].

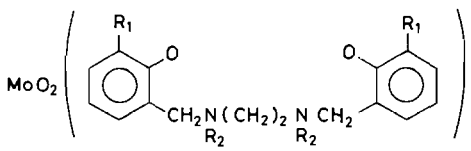

I, R_1 = H, R_2 = Me
II, R_1 = H, R_2 = Et
III, R_1 = t-Bu, R_2 = Me

The EPR spectra of frozen (77 K) solutions of reduced **I–III** exhibit extreme rhombicity, with exceptionally low $\langle g \rangle$ values and large $^{95,97}Mo$ hyperfine splittings (Fig. 1, Table I). Room temperature EPR spectra are correspondingly broad (~3.3 mT).

*The ^1H coupling refers to the strongly coupled protons.

TABLE I. Anisotropic EPR Parameters[a]

	g_1	g_2	g_3	^{95,97}Mo (mT)		
				A_1	A_2	A_3
$[MoO_2L]^-$ [b]	1.980	1.908	1.777	3.6	3.7	10.0
$[MoO(S)L]^-$ [b]	1.978	1.909	1.836	5.9	3.2	7.0

[a]Obtained directly from spectra, 77 K. [b]From Complex **III**, 0.10 M $[(n\text{-}Bu)_4N][BF_4]$, MeCN.

TABLE II. Isotropic EPR Parameters[a]

	$\langle g \rangle$	$\langle A \rangle$ (mT)		
		^{95,97}Mo	^1H	^{11}F
$[MoO_2L]^-$	1.885	5.5		
$[MoO(S)L]^-$	1.904	(5)[b]		
cis-MoO(OH)L	1.926	5.2	1.2	
cis-MoO(O^2H)L	1.927	5.2		
cis-MoO(SH)L	1.936	4.8	1.0	
cis-MoO(S^2H)L	1.935	4.8		
cis-MoOFL[c]	1.920	5.7		1.5
XO[d]			1.27	
SO[e]			0.95	0.53
NR[f]			1.20	
NR[g]			0.85	0.77

[a]Room temperature, 0.10 M $[(n\text{-}Bu_4)N][BF_4]$, MeCN. Except for *cis*-MoOFL, from Complex **III**. [b]Estimate only because of large line width of signal. [c]From Complex **I**. [d]Rapid type 1 signal [3]. [e]Low pH form [3]. [f]Spinach NR [2]. [g]*E. coli* NR [2].

Treatment of the reduced solutions with an equivalent of CF_3COOH gives room temperature EPR spectra typical of oxo-Mo(V) complexes (higher $\langle g \rangle$ values, and much narrower line widths) [7], except for the presence of doublets in both the $I = 0$ and $I = 5/2$ features. The same treatment with CF_3COO_2H in the presence of ^2H_2O results in collapse of the doublet structures, indicating the splitting arises from coupling of a single ^1H (Fig. 2, Table II). Addition of an equivalent of CF_3COOH followed by 5 equivalents of $[(n\text{-}Bu)_4N]F$ gives a new doublet at lower $\langle g \rangle$, exhibiting ^{19}F splitting [8]. These results are interpreted in Scheme 1. Similar reversible coupled electron–proton transfers involving pH depen-

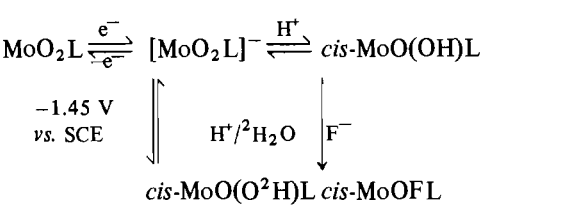

Scheme 1.

0020-1693/86/$3.50

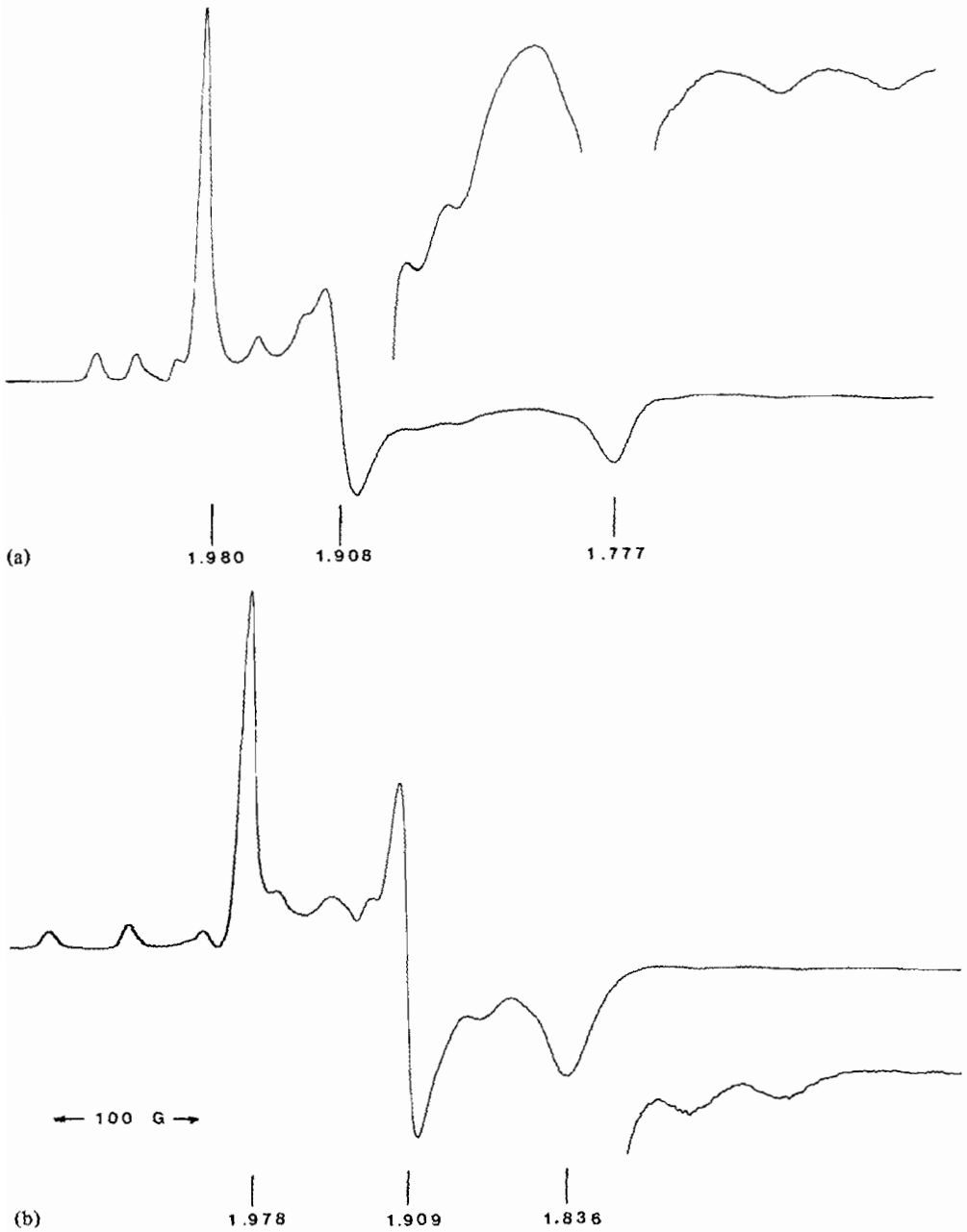

Fig. 1. X-band EPR signals in MeCN, 0.10 M $[(n\text{-}Bu)_4][BF_4]$, 77 K. (a) Electrolysis of 1.92×10^{-3} M **III** at −1.450 V (*vs.* SCE). (b) Addition of 1.92×10^{-3} M CF_3COOH followed by 3.27×10^{-2} M $[(n\text{-}Bu)_4N]SH$ to solution in (a).

dent equilibria occur in the Mo enzymes. Formulation of the initial one-electron reduced species of **I–III** as $[MoO_2L]^-$ is based on the reversible electrochemistry, unusual EPR signals, and reactions of the reduced species with H^+, SH^- and F^-*. The EPR spectra of both MoO(OH)L and MoOFL are consistent with *cis* structures [7, 8].

Treatment of the reduced solution of **III** with an equivalent of CF_3COOH followed by excess $[(n\text{-}Bu)_4N]SH$ results in the formation of a second broad

*The interpretation of frozen oxo-Mo(V) EPR spectra generally assumes octahedral or square pyramidal geometry with the *z* axis along the Mo-oxo bond, and the unpaired electron in the d_{xy} orbital, orthogonal to the oxo group [7]. This is the first report of dioxo-Mo(V), however, and *neither* the geometry nor the electronic structure is known; placement of the d_{xy} orbital in the plane of the two oxo groups with octahedral geometry, e.g., might result in considerably different EPR parameters. The extreme rhombicity indicates the presence of large spin orbit coupling.

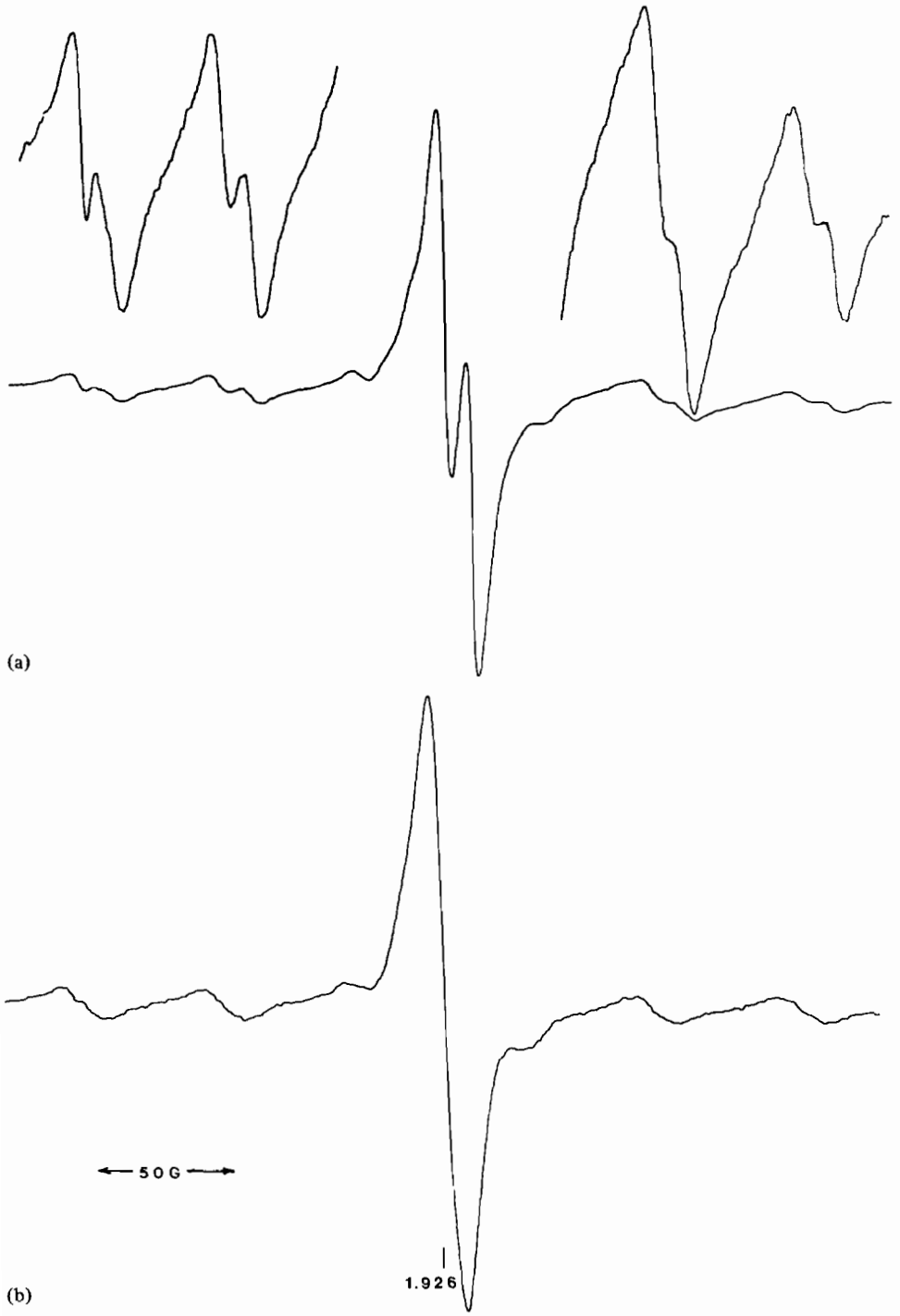

Fig. 2. X-band EPR signals in MeCN, 0.10 M $[(n\text{-}Bu)_4N][BF_4]$, room temperature. (a) Electrolysis of 2.00×10^{-3} M **III** at −1.450 V (*vs.* SCE) followed by addition of 2.00×10^{-3} M CF_3COOH. (b) Electrolysis as in (a) followed by addition of 2.00×10^{-3} M CF_3COO^2H and 1.11×10^{-2} M ^2H_2O.

room temperature signal, similar to that obtained in the reduction of MoO_2L, but with higher $\langle g \rangle$; the frozen spectrum is also similar to that obtained from initial reduction of MoO_2L, but with less rhombicity (Fig. 1, Table I). Subsequent treatment of this solution with CF_3COOH/H_2O gives a new signal exhibiting a doublet in the major features. This spectrum, however, is complicated by the appearance of a minor additional peak at higher $\langle g \rangle$. Identical treatment with $CF_3COO^2H/^2H_2O$ again results in collapse

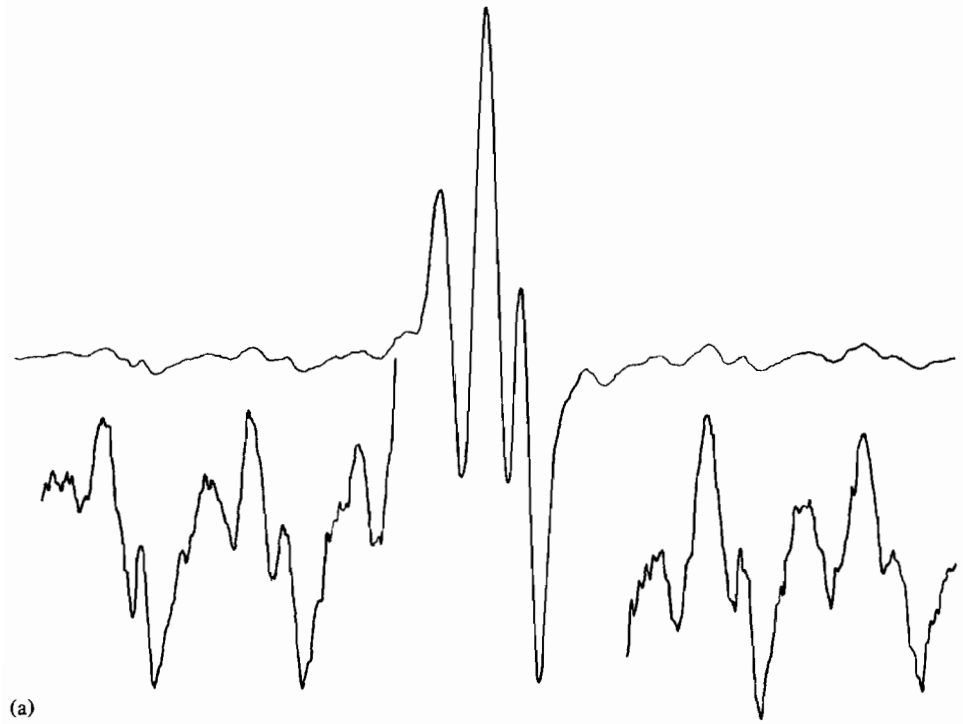

(a)

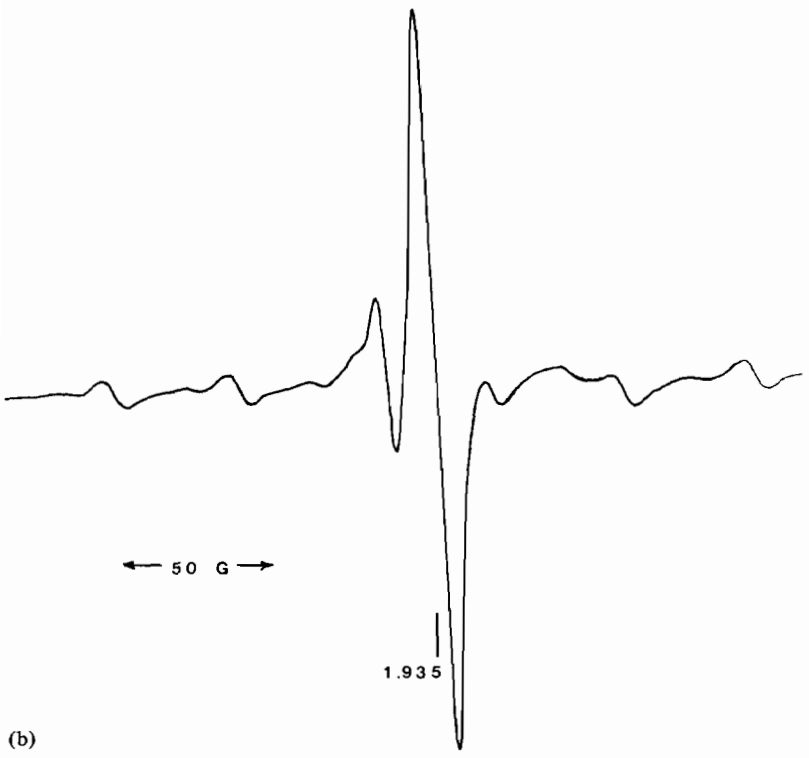

(b)

Fig. 3. X-band EPR signals in MeCN, 0.10 M $[(n\text{-}Bu)_4][BF_4]$, room temperature. (a) As in Fig. 1b, followed by addition of 5.89×10^{-3} M CF_3COOH and 2.38×10^{-2} M H_2O. [b] As in Fig. 1b, followed by addition of 5.89×10^{-3} M CF_3COO^2H and 7.91×10^{-3} M ^2H_2O.

$$cis\text{-MoO(OH)L} \xrightarrow{SH^-} [MoO(S)L]^- + H_2O$$

$$[MoO(S)L]^- \overset{H^+/H_2O}{\rightleftharpoons} cis\text{-MoO(SH)L}$$

$$\Big\Downarrow\Big\Uparrow \; {}^2H^+/{}^2H_2O$$

$$cis\text{-MoO(S}^2\text{H)L}$$

Scheme 2.

of the doublet features of the major signal, indicating the splitting arises from a single ^1H, while the minor peak is unaffected, (Fig. 3, Table II)*. These results are interpreted in Scheme 2. The protonated species are formulated as *cis*-MoO(SH)L rather than *cis*-MoS(OH)L since $\langle g \rangle$ is significantly higher than for *cis*-MoO(OH)L. Substitution of sulfido for oxo in Mo^VOCl_2L' to give Mo^VSCl_2L' (L' = hydrotris(3,5-dimethylpyrazolyl)borate) lowers $\langle g \rangle$ from 1.947 to 1.933 [9]. A similar result would be expected for *cis*-MoS(OH)L, since the equatorial ligands remain the same.

Comparison of the ^1H splittings for *cis*-MoO(OH)L and *cis*-MoO(SH)L with the corresponding parameters for SO, NR and XO strongly supports the presence of a *cis* OH (SO, NR) or SH(XO) ligand at the Mo centers of these enzymes (Table II). The ^{19}F splitting observed for *cis*-MoOFL is significantly larger, however, than that observed upon addition of F^- to SO and NR [10] (Table II).

*The anisotropic parameters for $[MoO_2L]^-$ and $[MoO(S)L]^-$ were obtained directly from the frozen spectra. For the other species, simulation and substitution with ^{95}Mo will be necessary to obtain accurate values of these parameters. Loss of OH^- from a small amount of MoS(OH)L in equilibrium with MoO(SH)L would give $[MoSL^+]$, possibly the source of the minor signal.

Acknowledgements

Thanks are expressed to J. H. Enemark for furnishing EPR data prior to publication. Financial support of this work by NIH Grant GM 08347 and NSF Grant CHE-8402136 is gratefully acknowledged.

References

1 S. P. Cramer, R. Wahl and K. V. Rajagopalan, *J. Am. Chem. Soc., 103,* 7721 (1981); S. P. Cramer, L. P. Solomonson, M. W. W. Adams and L. E. Mortenson, *J. Am. Chem. Soc., 106,* 1467 (1984); J. Bordas, R. C. Bray, C. D. Garner, S. Gutteridge and S. S. Hasnain, *Biochem. J., 191,* 499 (1980).
2 M. T. Lamy, S. Gutteridge and R. C. Bray, *Biochem. J., Biochem. J., 211,* 227 (1983); G. N. George, R. C. Bray, Nottom, R. J. Fido and E. J. Hewitt, *Biochem. J., 213,* 137 (1983); S. Gutteridge, S. J. Tanner and R. C. Bray, *Biochem. J., 175,* 869 (1978); S. P. Vincent and R. C. Bray, *Biochem. J., 171,* 639 (1978).
3 R. C. Bray, in L. J. Berliner and J. Reuben (eds.), 'Biological Magnetic Resonance', Vol. 2, Plenum, New York, 1980, p. 45.
4 T. Yamase, R. Sasaki and T. Ikawa, *J. Chem. Soc., Dalton Trans.,* 628 (1981); T. Yamase, *J. Chem. Soc., Dalton Trans.,* 1987 (1982).
5 P. Subramanian, J. T. Spence, R. Ortega and J. H. Enemark, *Inorg. Chem., 23,* 2564 (1984).
6 J. H. Enemark, unpublished results.
7 M. J. Scullane, R. D. Taylor, M. Minelli, J. T. Spence, K. Yamanouchi and J. H. Enemark, *Inorg. Chem., 18,* 3213 (1979).
8 P. T. Manoharan and M. T. Rogers, *J. Chem. Phys. 49,* 5510 (1968).
9 J. H. Enemark, unpublished results.
10 R. L. Bray, S. Gutteridge, M. T. Lamy and T. Wilkinson, *Biochem. J., 211,* 227 (1983); G. N. George, R. C. Bray, F. F. Morpeth and D. H. Boxer, *Biochem., J., 227,* 925 (1985).